Environmental Science and Ecotechnology 12 (2022) 100210

Contents lists available at ScienceDirect

Environmental Science and Ecotechnology

journal homepage: www.journals.elsevier.com/environmental-science-and-ecotechnology/

Short Communication

# The Nord Stream pipeline gas leaks released approximately 220,000 tonnes of methane into the atmosphere

Mengwei Jia [a, 1], Fei Li [a, 1], Yuzhong Zhang [b], Mousong Wu [a], Yingsong Li [a], Shuzhuang Feng [a], Hengmao Wang [a], Huilin Chen [c], Weimin Ju [a], Jun Lin [d], Jianwei Cai [d], Yongguang Zhang [a, e, f], Fei Jiang [a, g, h, *]

[a] Jiangsu Provincial Key Laboratory of Geographic Information Science and Technology, International Institute for Earth System Science, Nanjing University, Nanjing, Jiangsu Province, 210023, China
[b] Key Laboratory of Coastal Environment and Resources of Zhejiang Province, School of Engineering, Westlake University, Hangzhou, Zhejiang Province, 310030, China
[c] Joint International Research Laboratory of Atmospheric and Earth System Sciences, School of Atmospheric Sciences, Nanjing University, Nanjing, Jiangsu Province, 210023, China
[d] China Centre for Resources Satellite Data and Application, Beijing, 100094, China
[e] International Joint Carbon Neutrality Laboratory, Nanjing, Jiangsu Province, 210023, China
[f] Nantong Academy of Intelligent Sensing, Nantong, Jiangsu Province, 226000, China
[g] Jiangsu Center for Collaborative Innovation in Geographical Information Resource Development and Application, Nanjing, Jiangsu Province, 210023, China
[h] Frontiers Science Center for Critical Earth Material Cycling, Nanjing University, Nanjing, Jiangsu Province, 210023, China

ARTICLE INFO

*Article history:*
Received 15 October 2022
Received in revised form
24 October 2022
Accepted 24 October 2022

ABSTRACT

Sudden mega natural gas leaks of two Nord Stream pipelines in the Baltic Sea (Denmark) occurred from late September to early October 2022, releasing large amounts of methane into the atmosphere. We inferred the methane emissions of this event based on surface in situ observations using two inversion methods and two meteorological reanalysis datasets, supplemented with satellite-based observations. We conclude that approximately 220 ± 30 Gg of methane was released from September 26 to October 1, 2022.



In late September 2022, according to the Danish Energy Agency, several leaks were discovered in the submerged Nord Stream 1 and Nord Stream 2 gas pipelines in the Baltic Sea near Sweden and Denmark [1]. On the morning of September 26, a leak from the Nord Stream 2 pipeline was detected in a location (54.88° N, 15.41° E) to the southeast of the island of Bornholm, Denmark. That evening, the North Stream 1 pipeline also started to leak in two locations (55.54° N, 15.60° E and 55.56° N, 15.79° E) to the northeast of Bornholm (Fig. 1a). Although neither pipeline was transporting natural gas at the time of occurrence of the leaks, they still contained large amounts of pressurized methane, which was ejected and produced large bubbles on the sea surface (Fig. 1b). As the pressurized methane leaked through the broken pipe and moved toward the sea surface, the size of the bubbles increased as the surrounding pressure decreased. Upon reaching the sea surface, the vast bubbles disturbed the sea surface above the location of each rupture. The Planet, Landsat-8, GF5-02-AHSI, Sentinel-2, and Sentinel-1 satellites all acquired relatively precise imagery of the bubbles. From September 26 to October 1, bubbles with diameters of 0.5–0.7 km were observed by different satellite platforms (Fig. 1c). The Danish Energy Agency announced on October 2 that the gas leaks from the North Stream pipelines had terminated.

Methane, a more powerful greenhouse gas than carbon dioxide of equivalent mass, has contributed 1.2 W $m^{-2}$ to direct and indirect radiative forcing since industrialization, making it the second most important greenhouse gas concerning climate change [2]. Most scientists and policymakers globally have reached a consensus regarding the need to reduce and control methane emissions [3,4]. Because methane has a lifetime of approximately a decade, this sudden mega leak of methane is likely to aggravate the already

* Corresponding author. Jiangsu Provincial Key Laboratory of Geographic Information Science and Technology, International Institute for Earth System Science, Nanjing University, Nanjing, Jiangsu Province, 210023, China
*E-mail address:* jiangf@nju.edu.cn (F. Jiang).
[1] These authors contributed equally to this work.

https://doi.org/10.1016/j.ese.2022.100210

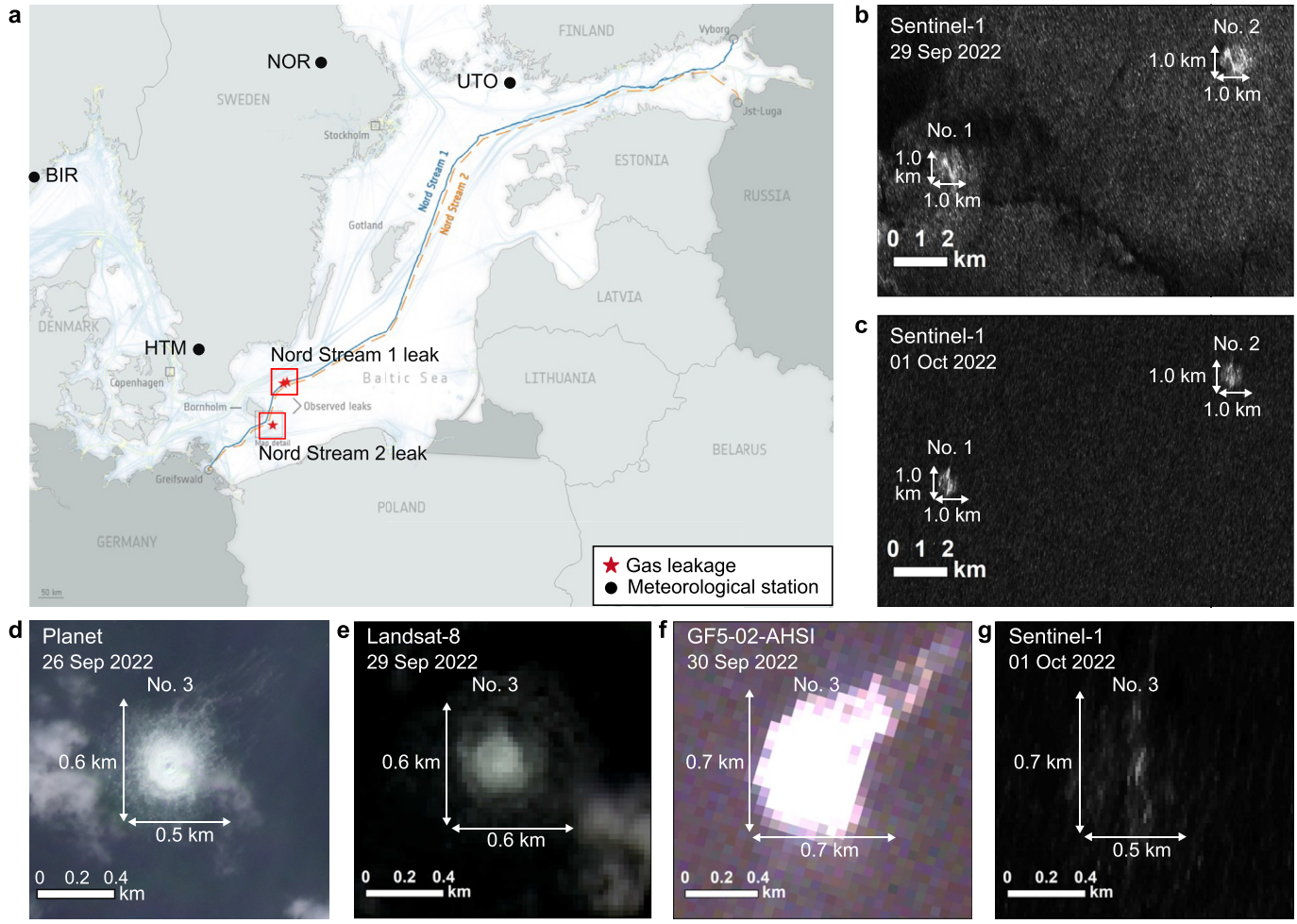


**Fig. 1.** a, Locations of leaks in the Nord Stream 1 and 2 pipelines. The black dots identify the Integrated Carbon Observation System (ICOS) sites of Birkenes (BIR), Hyltemossa (HTM), Norunda (NOR), and Utö—Baltic Sea (UTO), and the red stars represent the locations of the leaks detected on September 26, 2022. **b**–**g**, Remote sensing imagery of the escaping gas. **b**–**c**, The remote sensing images of the area of the Nord Stream 1 pipeline leak on September 29 (**b**) and October 1 (**c**), which were acquired by the Sentinel-1 satellite. **d**–**g**, The remote sensing images of the area of the Nord Stream 2 pipeline leak, acquired by the Planet (**d**), Landsat-8 (**e**), GF5-02-AHSI (**f**), and Sentinel-1 satellites (**g**), from September 26 to October 1, 2022. We use Coordinated Universal Time (UTC) throughout this paper.

severe global climate change situation. Therefore, quantifying the actual emissions associated with this incident is urgently required. Here, using in situ and satellite observations, we applied a multi-source inversion approach to estimate the rate of methane emission and its variation at the leak site of the North Stream natural gas transmission pipeline and to quantify the total mass of leaked methane.

The methane concentrations monitored by the Integrated Carbon Observation System (ICOS) at several sites in the southern Nordic region (Fig. 1a), and the transport of methane simulated by a plume model, confirmed that the leaks affected a large area of Europe within a short period following their initial occurrence. Methane concentrations at the Birkenes (BIR), Hyltemossa (HTM), Norunda (NOR), and Utö—Baltic Sea (UTO), located to the north of the leak area, all presented multiple notable peaks and sharp fluctuations in methane concentration from September 27 (Fig. 2a). The simulation of the in-line plume rise calculation in the Community Multiscale Air Quality (CMAQ) model (Methods S1 in the Supplementary) indicated that the methane was transported to both UTO and NOR by early on September 27 (Fig. 2b and c). Then, the plume shifted westward from late September 27 to 28, and the methane reached the sea to the west of Norway after passing across HTM and BIR (Fig. 2d and e). The plume then reached the United Kingdom by September 28, and further westward transport continued on September 29. Although the magnitude of the fluctuations on September 29 was much lower than that on the previous two days, HTM still experienced marked fluctuations in methane concentration (Fig. 2f and g). The methane leakage rate is likely to gradually decrease as the pipeline gas pressure drops. The leak continued on September 30 and affected regions to the east of the leak area. The peak methane concentration at the Nordic sites decreased as the leak intensity diminished, and the direction of transport shifted. In comparison with the period before the leaks, the highest hourly methane concentration during September 27—30 at HTM, BIR, NOR, and UTO increased by 317, 351, 306, and 63 ppb, representing increases of 17.4%, 15.7%, 15.1%, and 3.1%, respectively, in relation to the pre-leak levels.

Although optical satellites can provide information on the radius of methane bubbles on the water surface, such data are not equivalent to methane emission rate. Here, we used three atmospheric inversion methods (M1, M2, and M3) of different observations to quantify the methane emissions. M1 and M2 used different atmospheric transport models (i.e., the Weather Research and Forecasting (WRF)-the Community Multiscale Air Quality model

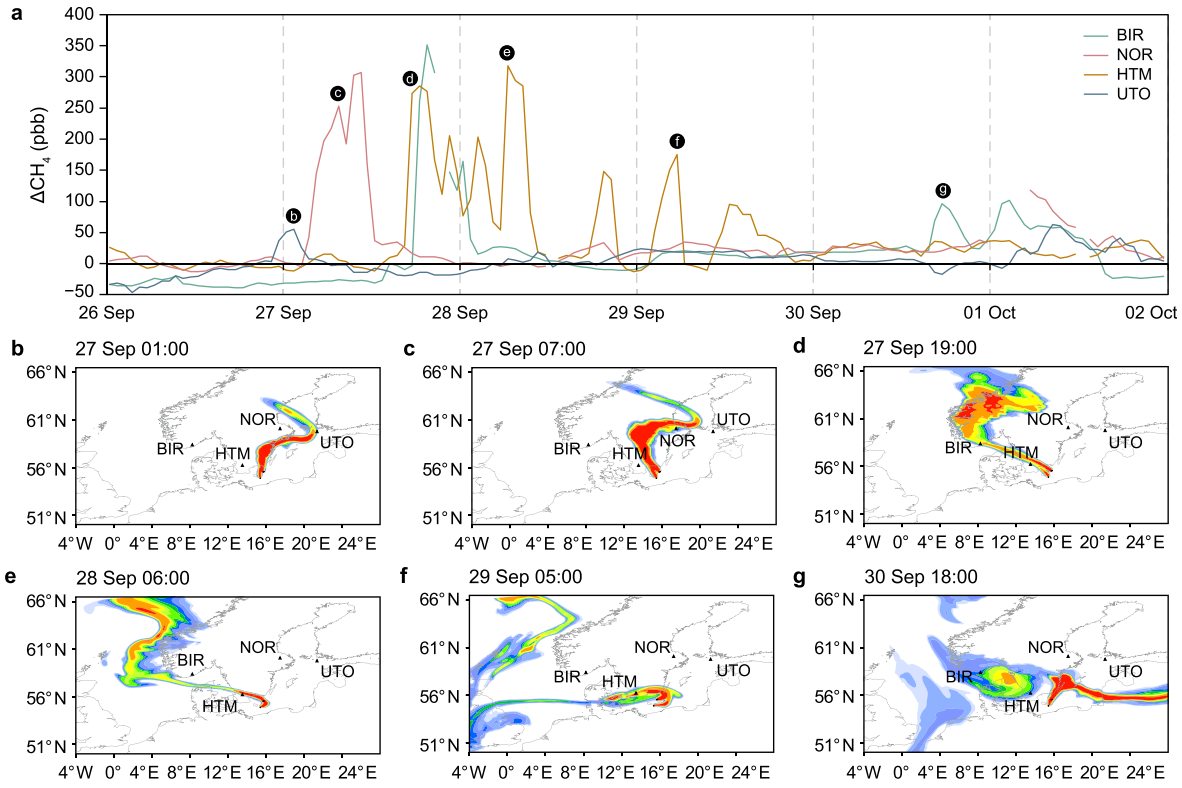


**Fig. 2.** a, Methane increments at the four ICOS sites of BIR, HTM, NOR, and UTO. **b**–**g**, Plume simulations at peak concentration from September 26 to October 1, 2022.

(CMAQ) [5] and Stochastic Time-Inverted Lagrangian Transport (STILT) models [6,7]) and meteorological information (i.e., the Fifth Generation Atmospheric Reanalysis of the Global Climate (ERA5) [8] and Global Forecast System (GFS) [9] datasets), thereby providing an assessment of transport errors. M3 mapped methane emission from the sea surface with spaceborne imaging spectrometers by employing a simple Beer's law retrieval [10] and integrated mass enhancement method (IME) [11].

In M1 and M2, we estimated the temporal variation of methane emissions from these leaks using in situ concentration measurements from the four ICOS sites (BIR, HTM, NOR, and UTO) [12–15]. We determined the background methane level at each of the four sites as the median of all September observations before September 26 and computed the methane enhancement by removing the background value from the raw data.

In M1, we assumed an initial emission rate of 1000 t $h^{-1}$, and we used the WRF-CMAQ model to calculate the hourly concentration contribution from September 26 to October 1 for each 12-h emission period at each station. The WRF-CMAQ simulation was driven by 0.25° × 0.25° global meteorological fields from ERA5 with a spatial resolution of 9 km. The methane emission rate for each time period was then derived by applying an initial guess (1000 t $h^{-1}$) with the ratio of the simulated concentration contribution and the observed methane enhancement. We also examined the uncertainty of the emission estimates using alternative background levels.

In M2, we used the STILT model to characterize atmospheric transport. The STILT simulation was driven by 0.25° × 0.25° global meteorological fields from the National Centers for Environmental Prediction (NCEP) operational GFS analysis with a spatial resolution of 0.1° × 0.1°. We first derived the sensitivity of methane enhancement at each ICOS site to the emission rate based on the STILT simulation, which computed the movement of particles released from the leak. Then, we solved a Bayesian inverse problem to estimate the hourly methane emission fluxes (posterior emissions) [16]. We assumed a prior emission of zero from the leaks with a Gaussian prior error of 2500 t $h^{-1}$ and a Gaussian observation error of 30 ppbv, mainly attributable to uncertainty in the transport model. We also calculated posterior errors to assess the uncertainties of this inversion.

In addition to in situ observations, methane monitoring data from satellites were used for comparisons. In M3, we detected the methane plume by using Landsat-8 and Sentinel-2 satellites. The first step is the derivation of the methane concentration enhancement ($\Delta X_{CH_4}$) map. The applied $\Delta X_{CH_4}$ retrieval method is based on the simple band ration between a band sensitive to methane and a spectrally close band with no sensitivity (or minimum sensitivity). In Landsat-8, we have used band B7 as the band with the highest sensitivity and B6 as the closest band with the lowest sensitivity and in Sentinel-2 bands B12 and B11 in the same order. Once we obtained the $\Delta X_{CH_4}$ map, we performed a plume mask to select methane plume pixels and quantify the emission. Finally, we converted the selected pixels into flux rate ($Q$) by applying the IME method.

Using the methods described above (details refer to Methods S2–S4), we performed temporal inversions for the leakage. The temporal resolutions of M1 and M2 are 12 and 1 h, respectively. For comparison, we averaged the results of M2 over 12 h to report methane emission rates. Both M1 and M2 emission rates show an overall trend of reduction as the leakage developed (Fig. 3c), consistent with the trend of the inversion results produced by the Norwegian Institute for Air Research [17]. Additionally, the results for both M1 and M2 show strong agreement with the increase in the number of leakage points. The two leaks in Pipeline 1 started leaking approximately half a day to a full day later than the leak in Pipeline 2. Both M1 and M2 present a significant increase in

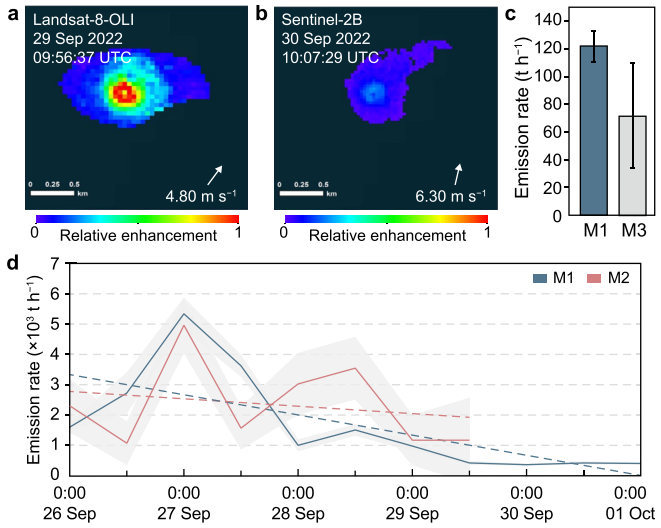


**Fig. 3.** Relative enhancements based on satellite observations (**a**–**b**) and inversion results of methane emissions from in situ observations (**c**–**d**). Relative enhancement of the plume at the Nord Stream 2 leak site was calculated from the Landsat-8-OLI satellite on September 29 (**a**) and from the Sentinel-2B satellite on September 30 (**b**). **c**, The emission rate of individual leak sites on September 30 in M1 (blue) and M3 (gray), with the black line indicating the uncertainty range. **d**, Inversion results of methane emissions based on in situ observations. The solid line and the dashed line indicate the 12-h average and the linear fit of the emission rate, respectively. The gray shaded area indicates uncertainty.

emission rate on the morning of September 27. During the night of September 28, another leak occurred in Pipeline 1, and the emission rate rebounded. The estimated methane emission rate during September 26–28 using M1 and M2 ranged from 1005 to 5340 t $h^{-1}$ (M1) and 810–4961 t $h^{-1}$ (M2). The Copernicus Atmosphere Monitoring Service estimated the leak to be 175 Gg during the first two days of the incident (September 26–27) [18], which is slightly higher than our M1 and M2 estimates of 159 ± 21 and 119 ± 39 Gg during the same period (Table S1). Although the models and algorithms of M1 and M2 are different, the estimation of the total leakage is highly consistent, suggesting the reliability of our estimates. Besides, we performed forward simulations using the inverse emission results of M1 and M2, respectively (Figs. S2–S3), and the simulation can reasonably capture the methane enhancements observed at the four ICOS sites, which also validates the reliability of our results. Because M1 provides a longer time series, we used the M1 method to assess the total amount of methane emission during the entire incident. The total amount of methane leakage was estimated to be 220 ± 30 Gg before noon on October 1; that is, slightly higher than the estimation of the Norwegian Institute for Air Research (56–155 Gg) for the same period [17]. This might be attributable to the fact that the two estimations were based on simulations with different resolutions and different observations.

We also estimated the total methane emission using the pipe dimensions and changes in gas pressure. First, from the inner diameter (1.153 m) and length (1224 km) of the circular pipeline [19], we calculated the pipeline volume as 1.27 × $10^6$ $m^3$. Next, using the Natural Gas Density Calculator (https://www.unitrove.com/engineering/tools/gas/natural-gas-density), and based on the change in gas pressure (drop from 105 bar to 7 bar, see https://www.archyde.com/from-105-to-seven-bar-pressure-drop-in-nord-stream-2/), gas temperature (assumed to be 5 °C), and methane content (assumed to be 96.5%) in the pipeline, we calculated that the change of gas density in the pipeline was 93.583 kg $m^{-3}$. Finally, we calculated that approximately 115 Gg of methane leaked from each pipeline, giving a total of approximately 230 Gg from the two pipelines. Our inversion (220 ± 30 Gg) is very consistent with this calculation.

We further used two satellite images acquired by the Landsat-8-OLI and Sentinel-2B on September 29 and 30 to detect methane plumes over the Nord Stream 2 leak (Fig. 3a and b). For example, the result derived from Sentinel-2B showed that $\Delta X_{CH_4}$ was as high as approximately 15 ppm (https://twitter.com/MethaneData/status/1575928109463138304). According to the methods of Varon et al. [11], the methane point emission could have been approximately 72 ± 38 t $h^{-1}$. Although this emission rate is generally comparable with our results derived from atmospheric inversions (i.e., 122 ± 11 t $h^{-1}$ for the morning of September 30 (Fig. 3c)), it probably includes significant uncertainties attributable to two possible reasons. First, the spectral reflectance of the bubbles (very bright) might have contributed a large fraction of the reflected radiance, which is difficult to separate from the absorption of methane in the SWIR band. This probably leads to an overestimation of $\Delta X_{CH_4}$. Second, the satellite images missed a large part of the plume (the one over water) because water can absorb most of the sunlight in the SWIR range used for methane retrieval, especially in relation to the nadir observations of Landsat-8 and Sentinel-2. Thus, considering the influence of both bubble reflectance and water absorption, the relative enhancement of the two plumes detected over the Nord Stream 2 leak is shown in Fig. 3a and b.

Fortunately, the impact of the sea surface can be reduced for satellites in the sun-glint observation mode [20], which was the case for the GHGSat observations acquired on September 30. From measurements over the Nord Stream 2 leak, GHGSat estimated a methane emission rate of 79 t $h^{-1}$ at 10:28:12 UTC and 29 t $h^{-1}$ at 12:56:32 UTC. However, this large variation in emission rate within a 3-h period might indicate the influence of different sunlight intensities at the time of each acquisition. Much more work is needed in the future to investigate problems with regard to satellite observations, particularly the avoidance of possible artifacts attributable to the impact of bubbles.

After the sudden mega leaks of the two Nord Stream pipelines, satellite and in situ observations showed signals of significant methane emission. Results showed that the ambient atmospheric methane concentration in the southern Nordic region increased by up to 17%. Using multisource observations interpreted with different inversion systems, we estimated the evolution of the methane emission rate during this incident. We found a leakage rate of approximately 5000 t $h^{-1}$ in the early stage of the event and an overall gradual decrease in the emission rate thereafter. The total amount of methane leaked was estimated to be 220 ± 30 Gg before noon on October 1. This figure surpasses the Aliso Canyon gas leak (100 Gg) that occurred in California in 2015 [21], making the Nord Stream leak the largest gas leak ever reported. In IPCC (AR6) [2], the 100-year global warming potential compared to carbon dioxide of methane ranges from 27.2 to 29.8. This means that 220 Gg of methane has the same global warming potential as 6200 Gg of carbon dioxide. Using the 2019 anthropogenic methane emission data of the World Resources Institute (all converted to carbon dioxide equivalent ($MtCO_2e$)) [22], the 220 ± 30 Gg of methane is about 0.08% and 85% of global and Danish annual anthropogenic methane emissions, respectively, and comparable to the annual anthropogenic methane emission in Austria (6.20 $MtCO_2e$). Uncertainties in the prior error for emissions, background levels, the small size of the spill area, bubble reflectance, and the high water absorption caused unavoidable uncertainties in the derived results.

## Declaration of competing interest

The authors declare that they have no known competing financial interests or personal relationships that could have appeared to influence the work reported in this paper.

## Acknowledgments

The work was supported by the National Key R&D Program of China (Grant No: 2021YFB3901001), Research Funds for the Frontiers Science Center for Critical Earth Material Cycling, Nanjing University (Grant No: 090414380031), and National Natural Science Foundation of China (Grant No: 42007198). We are grateful for being granted access to the Integrated Carbon Observation System methane observation datasets. We would like to thank the European Space Agency and the United States Geological Survey for the access to the Sentinel-2 and Landsat-8 datasets. We thank the Ministry of Ecology and Environment Center for Satellite Application on Ecology and Environment and China Center for Resources Satellite Data and Application for the access to the GF5-02-AHSI data. We are also grateful to the High-Performance Computing Center (HPCC) of Nanjing University for performing the numerical calculations reported in this paper on its blade cluster system.

## Appendix A. Supplementary data

Supplementary data to this article can be found online at https://doi.org/10.1016/j.ese.2022.100210.

## References

[1] Danish Energy Agency. https://ens.dk/en/press/leak-north-stream-2-baltic-sea. (Accessed 12 October 2022).
[2] P. Arias, N. Bellouin, E. Coppola, R. Jones, G. Krinner, J. Marotzke, V. Naik, M. Palmer, G. Plattner, J. Rogelj, M. Rojas, J. Sillmann, T. Storelvmo, P. Thorne, B. Trewin, K. Achutarao, B. Adhikary, R. Allan, K. Armour, G. Bala, R. Barimalala, S. Berger, J.G. Canadell, C. Cassou, A. Cherchi, W. Collins, W. Collins, S. Connors, S. Corti, F. Cruz, F. Dentener, C. Dereczynski, A. Di Luca, A. Diongue Niang, P. Doblas-Reyes, A. Dosio, H. Douville, F. Engelbrecht, V. Eyring, E. Fischer, P. Forster, B. Fox-Kemper, J. Fuglestvedt, J. Fyfe, N. Gillett, L. Goldfarb, I. Gorodetskaya, J. Gutierrez, R. Hamdi, E. Hawkins, H. Hewitt, P. Hope, A. Islam, C. Jones, D. Kaufmann, R. Kopp, Y. Kosaka, J. Kossin, S. Krakovska, J. Li, J. Lee, V. Masson-Delmotte, T. Mauritsen, T. Maycock, M. Meinshausen, S. Min, T. Ngo Duc, F. Otto, I. Pinto, A. Pirani, K. Raghavan, R. Ranasighe, A. Ruane, L. Ruiz, J. Sallée, B. Samset, S. Sathyendranath, P. Monteiro, S. Seneviratne, A. Sörensson, S. Szopa, I. Takayabu, A. Treguier, B. van den Hurk, R. Vautard, K. Von Schuckmann, S. Zaehle, X. Zhang, K. Zickfeld, in: V. Masson-Delmotte, P. Zhai, A. Pirani, S. Conners, C. Péan, S. Berger, N. Caud, Y. Chen, L. Goldfarb, M. Gomis, M. Huang, K. Leitzell, E. Lonnoy, J. Matthews, T. Maycock, T. Waterfield, O. Yelekçi, R. Yu, B. Zhou (Eds.), Climate Change 2021: the Physical Science Basis" in Contribution of Working Group I to the Sixth Assessment Report of the Intergovernmental Panel on Climate Change, Cambridge Univ. Press, 2021.
[3] D. Shindell, J. Kuylenstierna, E. Vignati, R. van Dingenen, M. Amann, Z. Klimont, S. Anenberg, N. Muller, G. Janssens-Maenhout, F. Raes, J. Schwartz, G. Faluvegi, L. Pozzoli, K. Kupiainen, L. Höglund-Isaksson, L. Emberson, D. Streets, V. Ramanathan, K. Hicks, N. Oanh, G. Milly, M. Williams, V. Demkine, D. Fowler, Simultaneously mitigating near-term climate change and improving human health and food security, Science 335 (2012) 183–189, https://doi.org/10.1126/science.1210026.
[4] R. Alvarez, S. Pacala, J. Winebrake, W. Chameides, S. Hamburg, Greater focus needed on methane leakage from natural gas infrastructure, Proc. Natl. Acad. Sci. U.S.A. 109 (2012) 6435–6440, https://doi.org/10.1073/pnas.1202407109.
[5] D. Wong, J. Pleim, R. Mathur, F. Binkowski, T. Otte, R. Gilliam, G. Pouliot, A. Xiu, D. Kang, WRF-CMAQ two-way coupled system with aerosol feedback: software development and preliminary results, Geosci. Model Dev. (GMD) 5 (2012) 299–312, https://doi.org/10.5194/gmd-5-299-2012.
[6] J. Lin, C. Gerbig, S. Wofsy, A. Andrews, B. Daube, K. Davis, C. Grainger, A near-field tool for simulating the upstream influence of atmospheric observations: the Stochastic Time-Inverted Lagrangian Transport (STILT) model, J. Geophys. Res. Atmos. 108 (2013) 4493, https://doi.org/10.1029/2002JD003161.
[7] C. Gerbig, J. Lin, S. Wofsy, B. Daube, A. Andrews, B. Stephens, P. Bakwin, C. Grainger, Toward constraining regional-scale fluxes of $CO_2$ with atmospheric observations over a continent: 2. Analysis of COBRA data using a receptor-oriented framework, J. Geophys. Res. Atmos. 108 (2003) 4757, https://doi.org/10.1029/2003JD003770.
[8] European Centre for Medium-Range Weather Forecasts, ERA5 Reanalysis (0.25 Degree Latitude-Longitude Grid), Research Data Archive at the National Center for Atmospheric Research, Computational and Information Systems Laboratory, 2022, https://doi.org/10.5065/BH6N-5N20. (Accessed 2 October 2022).
[9] National Centers for Environmental Prediction/National Weather Service/NOAA/U.S. Department of Commerce, NCEP GFS 0.25 Degree Global Forecast Grids Historical Archive, Research Data Archive at the National Center for Atmospheric Research, Computational and Information Systems Laboratory, Boulder, Colo, 2015, https://doi.org/10.5065/D65D8PWK. (Accessed 5 October 2022).
[10] E. Sánchez-García, J. Gorroño, I. Irakulis-Loitxate, D. Varon, L. Guanter, Mapping methane plumes at very high spatial resolution with the WorldView-3 satellite, Atmos. Meas. Tech. 15 (2022) 1657–1674, https://doi.org/10.5194/amt-15-1657-2022.
[11] D. Varon, D. Jacob, J. McKeever, D. Jervis, B. Durak, Y. Xia, Y. Huang, Quantifying methane point sources from fine-scale satellite observations of atmospheric methane plumes, Atmos. Meas. Tech. 11 (2018) 5673–5686, https://doi.org/10.5194/amt-11-5673-2018.
[12] J. Hatakka, T. Laurila, R.I. ICOS, ICOS ATC NRT $CH_4$ Growing Time Series, Utö - Baltic Sea (57.0 M, 2022, 2022-03-01–2022-10-01, https://hdl.handle.net/11676/qvEmc25_1hehnOULK1RipRv0. (Accessed 1 October 2022).
[13] I. Lehner, M. Mölder, R.I. ICOS, ICOS ATC NRT $CH_4$ Growing Time Series, Norunda (58.0 M), 2022, 2022-03-01–2022-10-01, https://hdl.handle.net/11676/tBypcN3OYQS1lvnGLNNd31fk. (Accessed 1 October 2022).
[14] M. Heliasz, T. Biermann, R.I. ICOS, ICOS ATC NRT $CH_4$ Growing Time Series, Hyltemossa (70.0 M), 2022, 2022-03-01–2022-10-01, https://hdl.handle.net/11676/aZCMVSVg3y7hKv8R2q6oSq77. (Accessed 1 October 2022).
[15] C. Lund Myhre, S. Platt, C. Lunder, O. Hermansen, R.I. ICOS, ICOS ATC NRT $CH_4$ Growing Time Series, Birkenes (75.0 M), 2022, 2022-03-01–2022-10-01, https://hdl.handle.net/11676/8PtbXLo_YsgCCwdz0UvGl-bc. (Accessed 1 October 2022).
[16] G. Brasseur, D. Jacob, Modeling of Atmospheric Chemistry, Cambridge Univ. Press, 2017, https://doi.org/10.1017/9781316544754.
[17] Norwegian Institute for Air Research. https://www.nilu.com/2022/10/improved-estimates-of-nord-stream -leaks/. (Accessed 12 October 2022).
[18] The Copernicus Atmosphere Monitoring Service. https://atmosphere.copernicus.eu/cams-simulates-methane-emissions-nord-stream-pipelines-leaks. (Accessed 21 October 2022).
[19] General Background Paper on Nord Stream. https://www.nord-stream.com/press-info/library/. (Accessed 14 October 2022).
[20] N. Larsen, K. Stamnes, Methane detection from space: use of sunglint, Opt. Eng. 45 (2006), 016202, https://doi.org/10.1117/1.2150835.
[21] S. Conley, G. Franco, I. Faloona, D. Blake, J. Peischl, T. Ryerson, Methane emissions from the 2015 Aliso Canyon blowout in Los Angeles, CA, Science 351 (2016) 1317–1320, https://doi.org/10.1126/science.aaf2348.
[22] Climate watch historical GHG emissions, Washington, DC: World Resources Institute, https://www.climatewatchdata.org/ghg-emissions?end_year=2019&gases=ch4&source=PIK&start_year=1850. (Accessed 21 October 2022).